Available online at www.sciencedirect.com
SCIENCE DIRECT®
Chemical Physics Letters 412 (2005) 171–175
CHEMICAL PHYSICS LETTERS
www.elsevier.com/locate/cplett

Charge transfer through chemisorbed organic molecules – Neutralization of ionization processes at local sites in the molecule

Junseok Lee [a], Ilya A. Balabin [b], David N. Beratan [b], Jae-Gook Lee [a], John T. Yates Jr. [a,*]

[a] *Department of Chemistry, Surface Science Center, University of Pittsburgh, Pittsburgh, PA 15260, USA*
[b] *Department of Chemistry, Duke University, Durham, NC 27708-0354, USA*

Received 19 May 2005
Available online 19 July 2005

Abstract

The charge transfer through chemisorbed molecules has been studied by using normally oriented pyridine and benzoate molecules, chemisorbed on the Cu(1 1 0) surface. They yield H^+ ions from the outer three C–H bond locations when ionized by electron impact. The local yield of these H^+ ions allows the determination of the rate of electron transport through the molecule from the molecular contact point to the ionization position, causing ion neutralization. A superexchange (molecule-assisted tunneling) electron transfer process is found to control the electron-transfer event.

The electrical conductivity of molecules is fundamentally related to the growing field of molecular electronics in which selected molecules are used to control charge flow in an electronic circuit of molecular dimensions. Central challenges in this field include assessing the tunneling characteristics of molecules (including the dependence of electron transmission on molecular position [1–3]) and determining the influence of molecular contacts on the electron transport process [4].

A chemisorbed organic molecule on an atomically clean single crystal surface is an ideal prototype system for the investigation of charge transfer through the molecule. The ionization of adsorbed organic molecules by electron impact (electron stimulated desorption – ESD), producing H^+ ions from C–H bonds, is thought to originate from excitation processes that lead to local hole production in the C–H bond region [5]. This leads to a Coulomb repulsion process that ejects H^+ ions along the C–H bond direction. The cross-section for the local ionization process is determined by two factors: (1) the efficiency of initial excitation; and (2) the efficiency of ion neutralization in final-state processes involving charge transfer from the surface to the departing H^+ ion [6]. Menzel, Gomer, and Redhead (MGR) [7,8], in their original reports on ESD, indicate that for an adsorbed molecule, process (1), should proceed with a cross-section of $\sim 10^{-16}\,cm^2$, as it does for gas phase molecules. Since the cross-section for H^+ formation from adsorbed organic molecules is much lower than $10^{-16}\,cm^2$, as will be shown below, the cross-section for H^+ ion formation must be controlled mainly by process (2), the electron transfer from the metal surface to the final state of the system. Such electron-transfer processes have been extensively investigated for chemisorbed atoms and small molecules *bound close to the surface*, where tunneling of electrons through vacuum to the departing positive ion is assumed to dominate in the final state neutralization effect [9]. In contrast to small adsorbed molecules, when larger chemisorbed organic molecules such as those studied here are ionized, *the outer C–H bonds yielding H^+ ions, are located so far from the surface that appreciable vacuum tunneling cannot occur, and neutralization can only take place by superexchange through the framework of the*

* Corresponding author. Fax: +1 412 624 6003.
E-mail addresses: jyates@pitt.edu, jyates@vms.cis.pitt.edu (J.T. Yates Jr.).

0009-2614/$ - see front matter © 2005 Elsevier B.V. All rights reserved.
doi:10.1016/j.cplett.2005.05.101

molecule itself. This Letter demonstrates that such molecule-assisted electron transmission occurs in two closely related chemisorbed molecules, pyridine and benzoate, on the Cu(1 1 0) surface. Thus, H^+ yields from the electronic excitation of chemisorbed molecules probe the electron transfer rates to specific molecular positions in the molecule, an issue of great interest in molecular electronics.

Fig. 1 shows the H^+ ion angular distributions from chemisorbed pyridine [10] and chemisorbed benzoate on the Cu(1 1 0) surface at 80 K. These measurements were made by the TOF-ESDIAD (time-of-flight electron stimulated desorption ion angular distribution) method [11]. In each case a 3-beam H^+ pattern is observed, originating from the outer C–H bonds at the 3, 4 and 5 positions on the aromatic ring. The two H^+ angular distribution patterns are accurately aligned parallel to different principal crystallographic directions, as shown in Fig. 1a, as a consequence of the surface bonding geometry of the adsorbed molecules (Fig. 1b). In each case, a more intense normal H^+ beam, originating from the 4-position on the aromatic ring, is observed, indicating that the axis of each molecule is normal to the surface. It is fortunate that other possible ionic dissociation products, of higher mass than H^+, are not observed, as shown in the time-of-flight distributions of Fig. 1c. The absence of positive ions other than H^+ is due to efficient neutralization of the slowly moving massive ionic fragments by charge exchange with the surface. The TOF measurements of H^+ ions originating

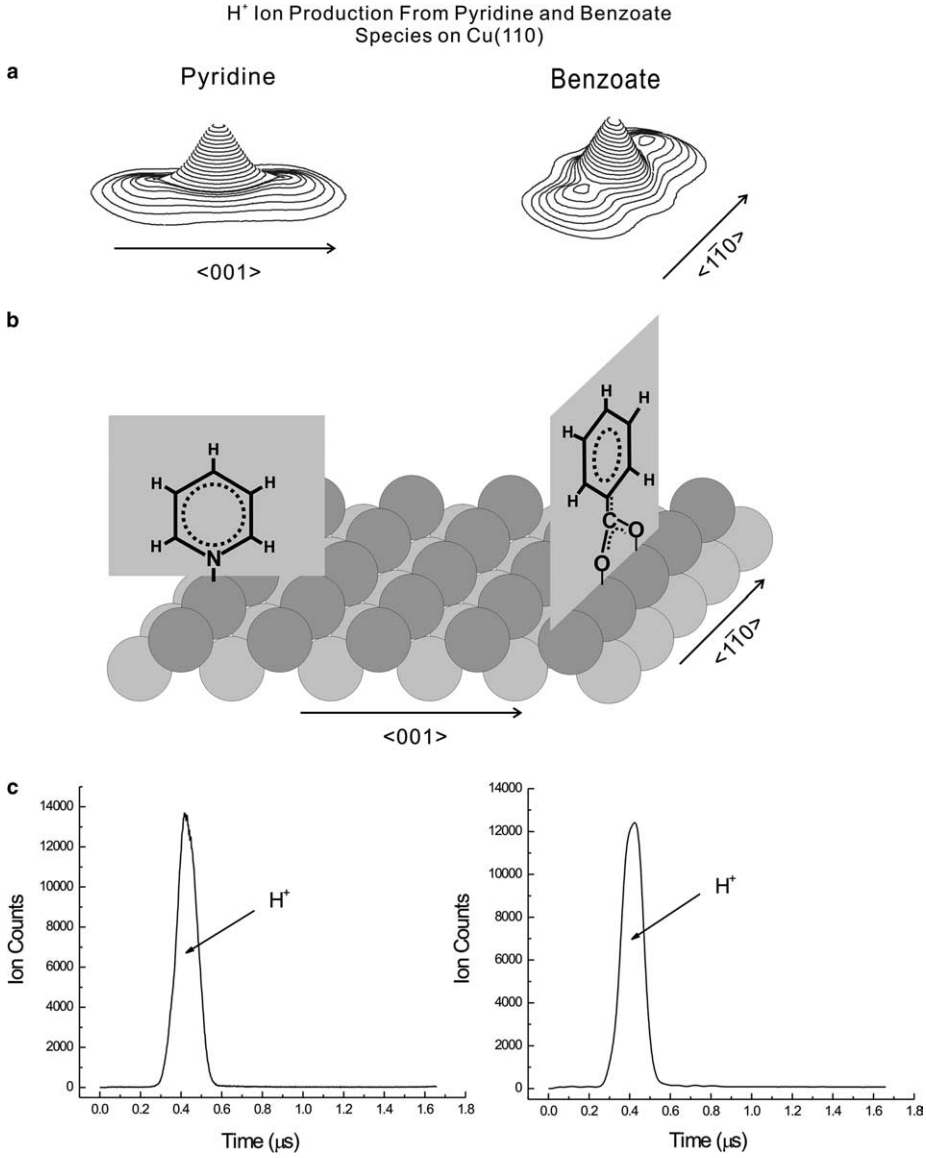

Fig. 1. (a) Comparison of the H^+ ionization angular distribution patterns of chemisorbed pyridine and benzoate on Cu(1 1 0) for electron stimulated desorption; (b) The molecular orientation of the two adsorbed molecules; (c) H^+ time-of-flight distribution for each molecule.

from the three C–H bond positions for each molecule indicate that the H^+ ion kinetic energy is identical for each position, with $E_{H^+} = 1.2$ eV.

By counting the number of H^+ ions produced at known incident electron currents during ESD from adsorbed layers of known coverage, we have calculated the cross-section for H^+ desorption from each C–H bond position for the two molecules using Eq. (1).

$$I^+_{(i)} = I_e Q^+_{(i)} N, \tag{1}$$

where $I^+_{(i)}$ is the H^+ count rate, I_e is the incident electron count rate derived from the measured current, $Q^+_{(i)}$ is the ionization cross-section from a particular ring position, i, to produce the observed H^+ ions, and N is the surface coverage of the adsorbed molecules (molecules/cm^2). The incident current, I_e, is measured at positive crystal bias to avoid secondary electron emission which would lower the observed collected current. The electron energy $V_e = 180$ eV.

Fig. 2a shows the geometrical situation for the two adsorbed molecules as well as the values of the local cross-section, $Q^+_{(i)}$, measured for H^+ ions originating from the 3, 4, and 5 positions of each molecule. In both cases, these values of $Q^+_{(i)}$ are in the range of 10^{-20}–10^{-21} cm^2. Fig. 2b also shows a cross-sectional slice through the middle of each H^+ pattern. It is observed that, for both molecules, the central H^+ beam ($i = 4$) is produced by an ionization process with a higher local cross-section, compared to the H^+ beams from the 3-and 5-positions, although the ratios in local cross-section differ for the two molecules. The relative yield of H^+ from the 4-position of pyridine, compared to that from the 3- and 5-positions, is almost independent of the incident electron energy over the range 100–600 eV (not shown). This indicates that the efficiency of the ionization process yielding H^+ from the three molecular positions is independent of the depth of initial ionization. This is likely because deep holes 'float upwards' rapidly to produce a common local repulsive final state at each molecular site, finally yielding an H^+ ion.

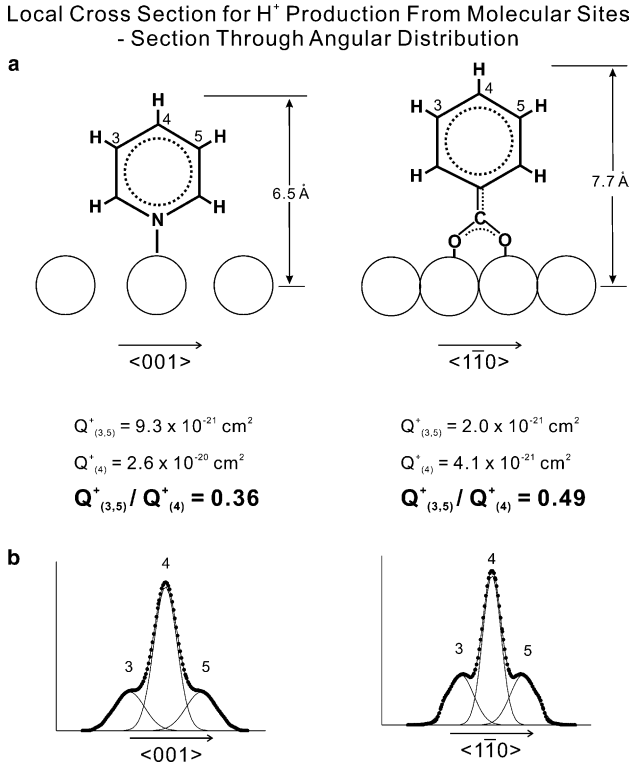

Fig. 2. (a) Comparison of the H^+ ionic cross-section for 3-, 4-, and 5-C–H molecular sites for chemisorbed pyridine and benzoate on Cu(110); (b) Cross-sectional cuts through the H^+ ion angular distributions.

Fig. 3 shows the total H^+ ionization cross-section, Q^+, for chemisorbed pyridine as a function of incident electron energy. A weak maximum, near 300 eV, is observed. The total ionization cross-sections measured for both chemisorbed pyridine and benzoate is about 5 orders of magnitude smaller than that found for gas phase molecules of the same type. For example, for benzene gas, at $V_e = 180$ eV, Q^+ (gas) $= 1 \times 10^{-15}$ cm^2 [12], while the value of $Q^+ = Q^+_{(3)} + Q^+_{(4)} + Q^+_{(5)}$ for the two chemisorbed aromatic molecules considered here is about 10^5 times smaller (10^{-20} cm^2).

The large difference in ionization cross-section of the chemisorbed vs. the gas phase organic molecules indicates that dominant electron-transport pathways exist from the metal that lead to H^+ neutralization for the two chemisorbed molecules. Excluding the improbable vacuum electron tunneling over distances of 7 Å, *the only pathway for electron transfer to the departing H^+ ion involves transport from the metal through the molecular framework to the hole at the molecular site being observed via H^+ ion yield, that is, a superexchange transport mechanism.*

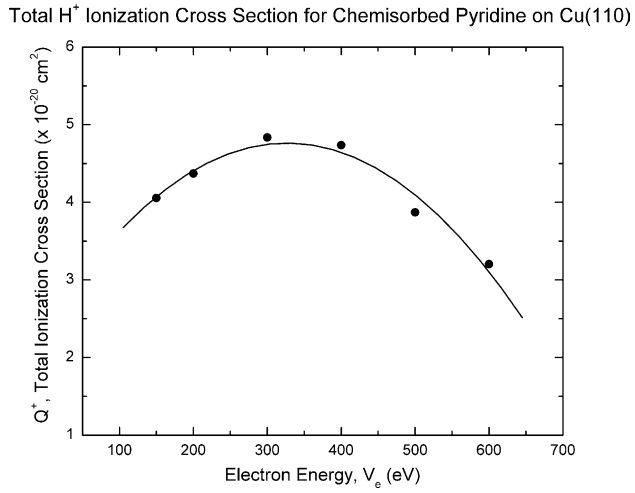

Fig. 3. Total cross-section for H^+ formation from chemisorbed pyridine on Cu(110) vs. electron energy.

We propose a model below to describe the H^+ ion desorption from chemisorbed aromatic organic molecules connected to the metal substrate by either a nitrogen or a carboxylate anchor group. The description is based on the MGR-like models [7–9,13–15], with the additional assumption that the transition to the dissociative state occurs in two steps: (1) initial electronic excitation leading to an electron–hole pair on the aromatic ring; and (2) hole localization on a C–H bond followed by an MGR-type desorption of the H^+ ion (The time scale for vacuum tunneling over 7 Å is microseconds, which is a million times too slow to quench the desorption). The model is applied below to describe the H^+ yields from pyridine and benzoate chemisorbed on the Cu(1 1 0) surface. Theoretical estimates are made for H^+ desorption cross-sections of the chemisorbed molecules vs. those for molecules in the gas phase. The calculated ratio of H^+ desorption yields from the C–H bond at position 4 vs. those at positions 3 and 5 are in reasonable qualitative agreement with experimental results.

Following the MGR models [7–9,13–16], we describe the molecule on the metal surface as an adsorbate (A)–substrate (M) system, where a hydrogen atom in a given C–H bond position is the 'adsorbate', and the carbon atom to which it is bonded is the 'substrate'. The system is in the ground state (M + A) initially, until an incident electron induces a Franck–Condon electronic transition to an electronically excited state. The transition occurs on the femtosecond time scale, and the system is described in a Born–Oppenheimer framework as functions of the reaction coordinate z that characterizes the relative motion of nuclei in A and M [9]. While the exact nature of the excited state is not known, it may include both σ- and π-orbitals mixed via thermal internal motion within the molecule.

After the excitation, the incident electron and the excited electron leave the system, and the remaining hole makes the electronic state dissociative [7–9,13–16], leading to the H^+ ion motion along z. The hole may be neutralized by another electron coming from the substrate. If that does not occur, it becomes energetically more favorable for the hole to localize at the C–H bond. After that, the MGR-like H^+ ion desorption may occur, or the ion may be 'recaptured'.

The total probability for H^+ ion emission from a C–H bond, therefore, is

$$P_{\mathrm{tot}} = \sigma_0 P_{\mathrm{loc}} P_{\mathrm{e}}, \tag{2}$$

where σ_0 is the cross-section of the interaction with the incident electrons, P_{loc} is the hole localization probability, and P_{e} is the ion-escape probability (lifetime τ_{e}) provided that the hole has already localized. For simplicity, we assume that the hole localization time scale is dominated by the change in the electronic state symmetry ($\pi \rightarrow \sigma$) and does not depend on the particular position of the C–H bond on the aromatic ring. The localization probability can then be roughly estimated as

$$P_{\mathrm{loc}} \propto \exp(-\tau_{\mathrm{loc}}/\tau_{\mathrm{ET}}), \tag{3}$$

where τ_{loc} is the localization time scale, and τ_{ET} is the time scale of the charge transfer from the substrate to the excited electronic state that quenches the hole. Since localization is primarily controlled by the H^+ ion motion driven by the repulsive potential resulting from the π–σ mixed excited state, τ_{loc} is considerably larger than the escape time τ_{e} after localization has occurred. The latter, as we show below, is of the same order of magnitude as the maximum ET rate ($\tau_{\mathrm{ET}} \sim 10^{-13}$–$10^{-14}$ s). To explain the experimentally observed data on the ratio for H^+ cross-sections for chemisorbed ($\sim 10^{-20}$ cm^2) vs. the gas phase ($\sim 10^{-15}$ cm^2) pyridine and benzoate species, we need τ_{loc} to be about 10 times larger than τ_{ET}, leading to P_{loc} values of about 10^{-4}.

The escape probability for H^+ from the C–H bonds can be estimated, as in the MGR models [9], as:

$$-\ln P_{\mathrm{e}} = \left(\frac{A}{b}\right)\left(\frac{M}{2B}\right)^{1/2} \exp(-z_0(a - b/2))F(p,u), \tag{4}$$

where M is the proton mass, z_0 is the initial (equilibrium) position of the adsorbate, $A\exp(-az)$ is the recapture rate (i.e., the quenching e^--transfer rate), and $B\exp(-bz)$ is the excited state potential energy function assumed to be a repulsive Born–Mayer form. $F(p, u)$ is the auxiliary function [9]; $p = (a/b)$, $u = b\,(z_{\mathrm{c}} - z_0)$, and

$$F(p,u) = \int_0^u \exp(-px)[1 - \exp(-x)]^{-1/2}\,\mathrm{d}x. \tag{5}$$

Avouris et al. [17] have analyzed ESD of hydrogen from Si(1 0 0) in a scanning tunneling microscope (STM). We use these same potential profiles to make qualitative estimates of the Born–Mayer potential parameters. The parameters are: $B \sim 6 \times 10^{-19}$ J, $b \sim 5$ Å^{-1}, $z_0 \sim 1.5$ Å, and $z_{\mathrm{c}} \sim 3.0$ Å.

The rates of charge transfer from the substrate to the aromatic ring and the C–H bonds at positions 3, 4, and 5 were estimated for chemisorbed pyridine and benzoate assuming a superexchange mechanism. The effective electronic couplings were computed at a tight-binding (extended Hückel) level [18], and the rate was assumed activationless [19]. The copper atoms covalently bonded to the molecule dominated the effective electronic coupling between the substrate and the molecule (The structure of pyridine and benzoate chemisorbed on Cu(1 1 0) was built using the program VMD (http://www.ks.uiuc.edu/Research/vmd) and the crystal structure from WebElements (http://www.webelements.com). The distances between the nitrogen atom in pyridine or the oxygen atoms in benzoate and the nearest substrate atoms were 1.93 and 2.08 Å, respectively, corresponding to the Cu–N and Cu–O distances typical for proteins [20]). The maximum charge transfer rates (parameter

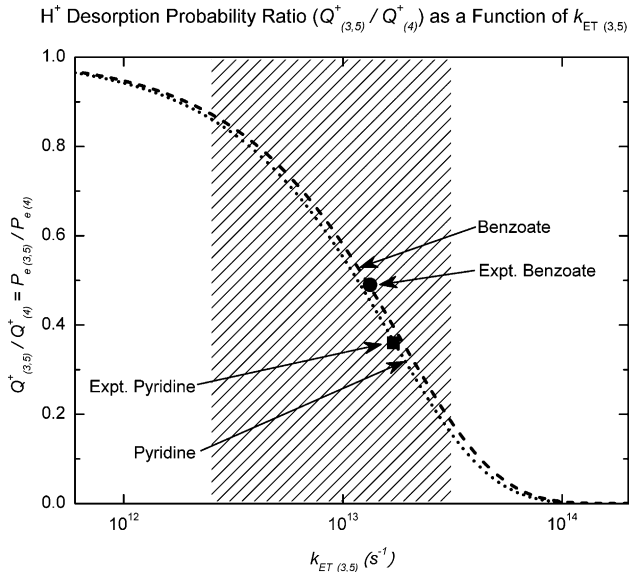

Fig. 4. H^+ desorption probability ratio from 3,5-positions compared to 4-position in chemisorbed aromatic compounds, as a function of k_{ET} to the 3,5-position.

$A = k_{ET}$) varied between 3×10^{12} and 3×10^{13} s^{-1}, and the rates to positions 3 and 5 were computed to be about five times faster than the rate to position 4. The distance decay (parameter a in the MGR models) was found to be about 0.7 $Å^{-1}$. The rates estimated in these calculations are consistent with simple exponential tunneling decay estimates [21].

Fig. 4 shows the ratio of P_e from positions 3 and 5 to P_e from position 4 as a function of the charge transfer rate (k_{ET}). Interestingly, the relative H^+ desorption probability is sensitive to the charge-transfer rate at values of k_{ET} of about 10^{13} s^{-1}, which are typical for pyridine and benzoate (and other small molecules). For larger molecules, the superexchange electron-transfer rate will be slower, leading to smaller quenching rates and similar desorption probabilities from all C–H bond positions.

In conclusion, we studied two representative large organic chemisorbed systems to understand charge transfer through the molecules. Information obtained from these studies may prove useful in designing molecular electronic devices. We find that the electron transmission between a metal and various molecular positions within a chemisorbed molecule may be measured indirectly. This is done by measuring the local ionization cross-section to produce H^+ ions from various C–H bond locations on the molecule. Electron transport pathways from the metal through the molecular framework are responsible for the reduction of H^+ yields from the outer C–H bonds. A superexchange process is consistent with the ratio of H^+ yields found from the different ring positions of chemisorbed pyridine and benzoate species.

Acknowledgments

We acknowledge with thanks, the support of our studies by the W.M. Keck Foundation to the Keck Center for Molecular Electronics within the Surface Science Center at the University of Pittsburgh. We also acknowledge support from the Japanese government through a NEDO Grant.

References

[1] M.H. Hettler, W. Wenzel, M.R. Wegewijs, H. Schoeller, Phys. Rev. Lett. 90 (2003) 076805;
J.W. Gadzuk, Surf. Sci. 342 (1995) 345.
[2] X.H. Qiu, G.V. Nazin, W. Ho, Phys. Rev. Lett. 92 (2004) 206102.
[3] V.J. Langlais, R.R. Schlittler, H. Tang, A. Gourdon, C. Joachim, J.K. Gimzewski, Phys. Rev. Lett. 83 (1999) 2809.
[4] F. Moresco, L. Gross, M. Alemani, K.-H. Rieder, H. Tang, A. Gourdon, C. Joachim, Phys. Rev. Lett. 91 (2003) 036601.
[5] D.E. Ramaker, J. Chem. Phys. 78 (1983) 2998.
[6] M. Nishijima, F.M. Propst, Phys. Rev. B 2 (1970) 2368.
[7] D. Menzel, R. Gomer, J. Chem. Phys. 41 (1964) 3311.
[8] P.A. Redhead, Can. J. Phys. 42 (1964) 886.
[9] R.D. Ramsier, J.T. Yates Jr., Surf. Sci. Rep. 12 (1991) 246.
[10] J.-G. Lee, J. Ahner, J.T. Yates Jr., J. Chem. Phys. 114 (2001) 1414.
[11] J. Ahner, D. Mocuta, R.D. Ramsier, J.T. Yates Jr., J. Vac. Sci. Technol. A 15 (1997).
[12] W. Hwang, Y.-K. Kim, M.E. Rudd, J. Chem. Phys. 104 (1996) 2956.
[13] D. Menzel, Nucl. Instr. and Meth. B 101 (1995) 1.
[14] P.R. Antoniewicz, Phys. Rev. B 21 (1980) 3811.
[15] P. Saalfrank, G. Boendgen, C. Corriol, T. Nakajima, Faraday Discuss. 117 (2000) 65.
[16] J.W. Gadzuk, L.J. Richter, S.A. Buntin, D.S. King, R.R. Cavanagh, Surf. Sci. 235 (1990) 317.
[17] Ph. Avouris, R.E. Walkup, A.R. Rossi, H.C. Akpati, P. Nordlander, T.-C. Shen, G.C. Abeln, J.W. Lyding, Surf. Sci. 363 (1996) 368.
[18] K. Yates, Hückel Molecular Orbital Theory, Academic Press, New York, 1978.
[19] I.A. Balabin, J.N. Onuchic, Science 290 (2000) 114.
[20] S. Yoshikawa, K. Shinzawa-Itoh, R. Nakashima, R. Yaono, E. Yamashita, N. Inoue, M. Yao, M.J. Fei, C.P. Libeu, T. Mizushima, H. Yamaguchi, T. Tomizaki, T. Tsukihara, Science 280 (1998) 1723.
[21] D.N. Beratan, J.N. Betts, J.N. Onuchic, Science 252 (1991) 1285.